https://doi.org/10.5194/gchron-2024-22
Preprint. Discussion started: 28 August 2024

Global analysis of in situ cosmogenic $^{26}Al/^{10}Be$ ratios in fluvial sediments indicates widespread sediment storage and burial during transport

Christopher T. Halsted[1], Paul R. Bierman[2], Alexandru T. Codilean[3], Lee B. Corbett[2], Marc W. Caffee[4]

[1]Department of Geosciences, Williams College, Williamstown, MA 01267, USA
[2]Rubenstein School of Environment and Natural Resources, Gund Institute for Environment, University of Vermont, , Burlington, VT 05405, USA
[3]School of Earth, Atmospheric and Life Sciences and Australian Research Council Centre of Excellence for Australian Biodiversity and Heritage (CABAH), University of Wollongong, Wollongong NSW 2522, Australia
[4]Department of Physics and Astronomy, Purdue University, West Lafayette, IN 47907, USA

Correspondence to: Christopher T Halsted (ch22@williams.edu)

Abstract. Since the 1990s, analysis of cosmogenic nuclides, primarily ^{10}Be, in quartz-bearing river sand, has allowed for quantitative determination of erosion rates at a basin scale. Paired measurements of in situ cosmogenic ^{26}Al and ^{10}Be in sediment are less common but offers insight into the history of riverine sediment moving down slopes and through drainage basins. Prolonged sediment burial (>10^5 years), a violation of assumptions underlying erosion rate calculations, is indicated by higher ^{26}Al-based than ^{10}Be-based erosion rates due to preferential loss of shorter-lived ^{26}Al by decay when quartz is shielded from cosmic rays.

Here, we use a global compilation of ^{26}Al and ^{10}Be data generated from quartz-bearing fluvial sediment samples (n = 624, including 121 new measurements) and calculate the discordance between erosion rates derived from each nuclide. We test for correlations between such discordance and topographic metrics for drainage basins, allowing us to infer the likelihood of sediment burial during transport in different geomorphic settings. We find that nearly half of samples (n = 276) exhibit discordance (> 1σ uncertainty) between erosion rates derived from ^{10}Be and ^{26}Al, indicating sediment histories that must include extended burial during residence on hillslopes and/or in the fluvial system after or during initial near-surface exposure. Physical basin parameters such as basin area, slope, and tectonic activity exhibit significant correlation with erosion rate discordance whereas climatic parameters have little correlation.

Our analysis suggests that $^{26}Al/^{10}Be$ erosion rate discordance occurs more regularly in basins larger than 1,000 km^2, particularly when such basins have low average slopes and are in tectonically quiescent terrains. Sediment sourced from smaller, steeper basins in tectonically active regions is more likely to have similar ^{10}Be and ^{26}Al erosion rates indicative of limited storage and limited burial during residence in the hillslope and fluvial sediment system. The data and analysis we present demonstrate that paired ^{26}Al and ^{10}Be analyses in detrital fluvial samples can provide a window into watershed processes, elucidating landscape behavior at different spatial scales and allowing a deeper understanding of both sediment routing systems and whether erosion rate assumptions are violated. Large lowland basins are more likely to transport detrital sediment that has experienced prolonged sediment storage and burial either on hillslopes and/or in fluvial networks; thus, erosion rates from such basins are lower limits due to nuclide decay during storage. Conversely, samples from smaller upland basins are more likely to provide reliable erosion rates.

https://doi.org/10.5194/gchron-2024-22
Preprint. Discussion started: 28 August 2024

1 Introduction

Fluvial sediments are a rich source of information about the upstream sediment routing system, which encompasses sediment generation, transport, and storage processes (Romans et al., 2016; Tofelde et al., 2021). For example, in situ cosmogenic ^{10}Be measurements in fluvial sediments are used to estimate basin-scale erosion rates, and the application of this method in thousands of drainage basins around the world has provided valuable insights into physical and climatic controls on erosion (von Blanckenburg, 2005; Codilean et al., 2022; Portenga and Bierman, 2011; Schaefer et al., 2022). However, such analyses assume an upstream sediment history in which material was generated through steady exhumation on hillslopes and then transported rapidly through fluvial networks, experiencing negligible storage while in transit (Bierman and Steig, 1996; von Blanckenburg, 2005; Granger et al., 1996; Granger and Schaller, 2014; Schaefer et al., 2022). Data by which to evaluate these assumptions are scarce.

Sediment grains in fluvial systems can have a wide range of idiosyncratic transport and storage histories potentially spanning more than 10^6 years in large basins (Wittmann et al., 2011), as shown by cosmogenic nuclide analyses in modern fluvial sediments (Fülöp et al., 2020; Repasch et al., 2020; Wittmann et al., 2011), volumetric and geochemical analyses of valley fills (Blöthe and Korup, 2013; Jonell et al., 2018; Munack et al., 2016), and sediment transport models (Carretier et al., 2020). These 'complex' sediment histories, along with the protracted sediment lag times, may confound reliable interpretation of upstream processes (Allen, 2008; Jerolmack and Paola, 2010). Sediment samples used for analysis of cosmogenic nuclides are typically amalgamations of thousands of grains, each of which has its own unique history.

Measuring in situ cosmogenic radionuclides with different half-lives is a promising approach for discerning fluvial sediment histories (Codilean and Sadler, 2021; Schaefer et al., 2022). Measuring the concentrations and calculating ratios between multiple cosmogenic radionuclides has provided insight into sediment provenance (e.g., Cazes et al., 2020) and storage histories (e.g., Wittmann et al., 2011; Fülöp et al., 2020; Ben-Israel et al., 2022) in large river systems. Such studies have helped test hypotheses about sediment dynamics in river basins, including that the integrated storage duration experienced by sediments on hillslopes and in floodplains is generally greater in larger basins (Wittmann et al., 2020a), in post-orogenic regions (Cazes et al., 2020; Struck et al., 2018), and in arid regions (Makhubela et al., 2019). However, such hypotheses have yet to be tested on a global scale and questions remain, such as whether sediment storage duration scales with physical and/or climatological basin attributes.

In this study, we compiled measurements of paired in situ ^{26}Al and ^{10}Be concentrations in detrital fluvial sediment from around the world (n = 624, including 121 new ^{26}Al measurements on archived samples with previously published ^{10}Be measurements) and explore how this nuclide pair can inform our understanding of sediment generation and transport dynamics. We account for localized differences in nuclide surface production ratios to facilitate comparison across the world and calculate morphometric and climatological parameters of sampled river basins to assess relationships between isotope concentrations and basin-scale landscape properties. Such a global description provides insight into the complexity of hillslope erosion and river sediment transport across a wide range of climatological, tectonic, morphometric, and lithologic regimes and allows us to evaluate the validity of assumptions in the widely-

https://doi.org/10.5194/gchron-2024-22
Preprint. Discussion started: 28 August 2024

used, basin-scale cosmogenic nuclide erosion rate method (von Blanckenburg, 2005; Granger and Schaller, 2014; Schaefer et al., 2022).

2 Background

2.1 Sediment system dynamics and landscape change

Fluvial sediments are products of sediment routing systems. These systems generally encompass regions of net sediment generation and export through bedrock weathering, regolith production, and sediment erosion from hillslope source zones (Allen, 2017). This detrital material is then transported by fluvial systems through riverine transfer zones and deposited in detrital sink zones (Schumm, 1977). Depending on the geometry of the riverine transfer zone, sediment storage may be transient (e.g., steep bedrock streams) or long lasting (e.g., lowland alluvial rivers). The extent and duration of storage in floodplains and sedimentary basins is an important control on weathering (e.g., Campbell et al., 2022; Dosseto et al., 2014) as well as on both the production of cosmogenic nuclides near the surface and the decay of those radionuclides if sediment is buried (Lal, 1991).

Understanding rates, controls, and dynamics of sediment generation and transport is important for quantifying landscape change over time and space (Allen, 2008; Romans et al., 2016). In many routing systems, river morphology (Langbein and Leopold, 1964; Leopold and Wolman, 1960) and floodplain volume (e.g., Otto et al., 2009) are determined by the sediment mass flux out of source zones, the rate of transit through transfer zones, and the accommodation space available for sediment storage. Changes to rates of sediment generation or transfer, primarily driven by tectonic or climatic forcings (Romans et al., 2016), can thus affect the behavior of both sediment-supplying hillslopes and riverine transfer zones. Identifying such changes over space and through time is an important objective of geomorphological research and has prompted the development of tracer and rate-determining detrital geochronologic methods including measurements of cosmogenic nuclides, fission tracks, fallout radionuclides, and U/Th/He in various mineral phases (Allen, 2017).

2.2 Interpreting landscape processes from cosmogenic nuclides

The application of cosmogenic nuclide analyses to fluvial sediments, first using single nuclides and later paired nuclides, has significantly advanced our understanding of geomorphology and sediment routing systems at a variety of spatial and temporal scales (e.g., Bierman and Nichols, 2004; von Blanckenburg, 2005; Codilean et al., 2021; Portenga and Bierman, 2011; Willenbring et al., 2013; Wittmann et al., 2020). Key to the interpretation of measured nuclide concentrations is a quantitative understanding of nuclide production and decay rates throughout the basin from which the sediment is derived. Outside of the arctic (Corbett et al., 2017), the ratio of ^{26}Al to ^{10}Be at production is ~6.8, but there are subtle influences of latitude and altitude on that ratio (Halsted et al., 2021). Nuclide production falls off exponentially with depth below Earth's surface such that once sediment is buried more than a meter or two, decay rather than production systematics controls the evolution of the ^{26}Al/^{10}Be ratio over time (Granger, 2006; Wittmann and von Blanckenburg, 2009).

https://doi.org/10.5194/gchron-2024-22
Preprint. Discussion started: 28 August 2024

2.2.1 Basin-scale erosion rates from single-nuclide measurements

Basin-scale erosion rates have been estimated across the world by measuring the concentration of a single cosmogenic nuclide, most often in situ ^{10}Be, in samples of amalgamated river sediment (Bierman and Steig, 1996; Brown et al., 1995; Codilean et al., 2022; Granger et al., 1996; Portenga and Bierman, 2011). Sediment grains accumulate ^{10}Be during exhumation and at the surface in source zones, with the nuclide concentration within grains being proportional to the residence time of grains on hillslopes (Heimsath et al., 1997; Jungers et al., 2009). When collecting a sample of fluvial sediment downstream, it is assumed that such a sample represents the average nuclide concentration in grains sourced from all sediment-generating hillslopes within a basin (Bierman and Steig, 1996; Granger et al., 1996; Brown et al., 1995).

Accuracy of basin-scale erosion rate calculations depends upon the validity of several assumptions about sediment generation and transport that cannot be tested with single-nuclide analyses: that sampled grains were steadily exhumed on hillslopes in sediment source zones, are well mixed, and are transported rapidly through fluvial networks such that nuclide production and decay in the transport zone is minimal (Bierman and Steig, 1996; Granger et al., 1996; Brown et al., 1995). This assumption is most likely to be valid if the volume of sediment stored in the system is small in comparison to the volume of sediment generated and transported through the system on timescales relevant to ^{10}Be production and decay (millennia; Granger et al., 1996).

2.2.2 Sediment routing dynamics from paired ^{10}Be and ^{26}Al

In situ ^{10}Be and ^{26}Al are the most common cosmogenic nuclide pair measured in river sediment, measurements having started in the late 1990s (Bierman and Caffee, 2001; Clapp et al., 2000, 2001, 2002; Heimsath et al., 1997; Nichols et al., 2002), both because of the relative ease of extracting this isotope pair from the same aliquot of quartz, and because of their contrasting half-lives (1.4 My and 0.7 My, respectively, Chmeleff et al., 2010; Korschinek et al., 2010; Nishiizumi, 2004). When sediment is buried, the shorter-lived ^{26}Al is preferentially lost as decay exceeds production and the ^{26}Al/^{10}Be ratio in quartz lowers over time (Balco and Rovey, 2008; Granger, 2006). ^{26}Al/^{10}Be ratios have been used as isotopic indicators of sediment storage and subsequent remobilization in catchments across the world, including arid (Bierman et al., 2001; Bierman and Caffee, 2001; Clapp et al., 2000, 2001, 2002; Kober et al., 2009), tropical (Campbell et al., 2022; Wittmann et al., 2011), and very large (Ben-Israel et al., 2022; Fülöp et al., 2020; Hidy et al., 2014; Wittmann et al., 2020b; Wittmann and von Blanckenburg, 2016) basins. However, in some studies, lowered ^{26}Al/^{10}Be ratios were attributed to laboratory errors (Insel et al., 2010; Walcek and Hoke, 2012; Hattanji et al., 2019) or incorporation of meteoric ^{10}Be (Moon et al., 2018) and disregarded.

In this study, sediment burial (and resulting preferential loss of shorter-live ^{26}Al by decay) is reflected by the discordance between erosion rates calculated from ^{10}Be (E_{Be}) and ^{26}Al (E_{Al}), the calculation of which normalizes spatial variations in the ^{26}Al/^{10}Be surface production rate and ratio and thus facilitates comparisons between basins across the world. If sediment is transferred from slopes into channels and transported through the channel network without extended burial, then erosion rates calculated from the concentration of each nuclide should be coincident ($E_{Be} = E_{Al}$). Discordance between erosion rates calculated from the two nuclides (unless it is caused by laboratory

https://doi.org/10.5194/gchron-2024-22
Preprint. Discussion started: 28 August 2024

errors) reflects preferential loss of ^{26}Al when and where decay exceeds production, in which case $E_{Be} < E_{Al}$. This occurs when sediment is stored below the surface (>2m) and for extended periods (>10^5 years) after initial surface exposure on hillslopes or in floodplains (Fig. 1).

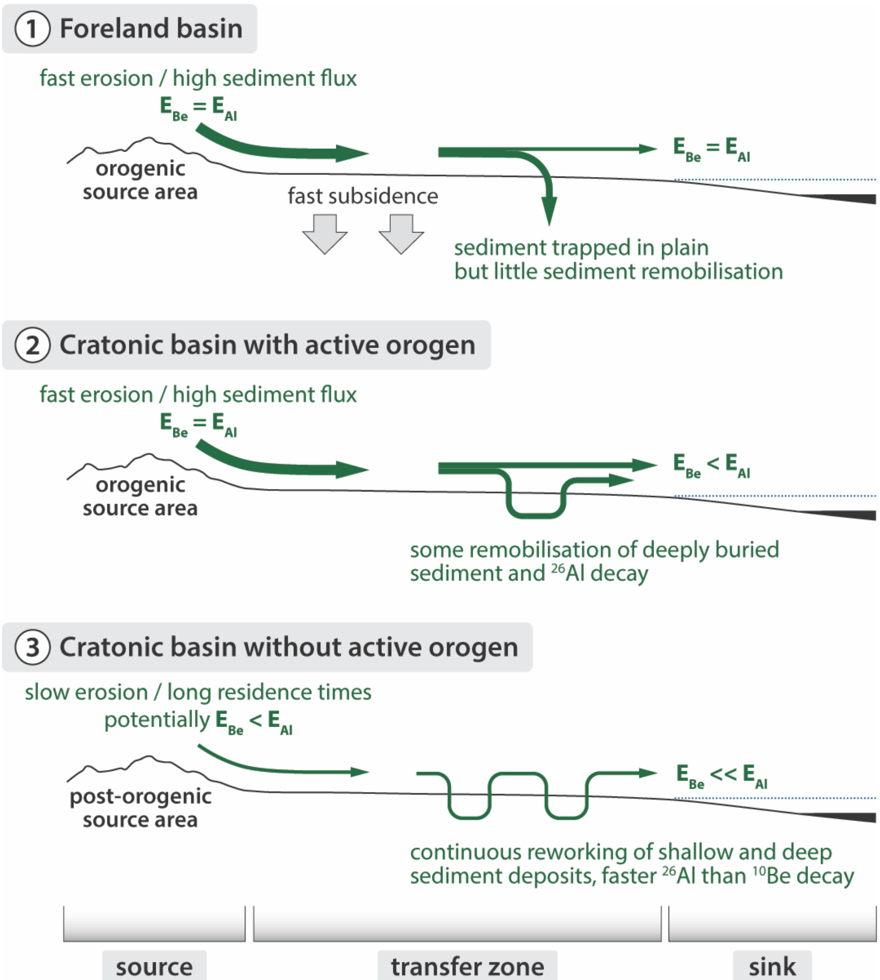

Figure 1: Effects of storage in sediment source and/or transfer zones on ^{10}Be and ^{26}Al-based erosion rates measured in detrital quartz grains. In Panel 1, rapid erosion rates in the source zone and limited remobilization of stored sediment in the transfer zone result in detrital sediment with concurrent erosion rates ($E_{Be}/E_{Al} = 1$). In Panel 2, rapid erosion rates in the source zone and some remobilization of stored sediment in the transfer zone result in detrital sediment with erosion rate discordance ($E_{Be}/E_{Al} < 1$), although prolonged sediment storage (>10^5 years) is necessary for erosion rate discordance to be measurable. In Panel 3, slow erosion rates in the source zone and remobilization of stored sediment in the transfer zone result in detrital sediment with substantial erosion rate discordance ($E_{Be}/E_{Al} << 1$). This figure is based on Figure 6 in Wittmann et al. (2016).

Floodplain sediment storage of <10^5 years has minimal effect on E_{Be}/E_{Al} ratios in sediment grains (Wittmann and von Blanckenburg, 2009), but during prolonged (>10^5 years) storage, especially at depths below which most nuclide by spallation occurs (> several hundred g cm^{-2}), a grain's E_{Be}/E_{Al} ratio will lower sufficiently that it can be

https://doi.org/10.5194/gchron-2024-22
Preprint. Discussion started: 28 August 2024

detected with confidence in samples containing moderate to high concentrations of these nuclides (Fig 1). In slowly-eroding terrains (<10 m My^{-1}), long subsurface sediment residence times on hillslopes can lead to erosion rate discordance in sediment source areas due to preferential ^{26}Al decay before regolith reaches the channel (Fig. 1; Makhubela et al., 2019; Struck et al., 2018). The rate of E_{Be}/E_{Al} lowering is depth-dependent, rates are higher with increased sediment burial depth as nuclide production rates decrease.

Re-introduction of stored sediment with low E_{Be}/E_{Al} ratios back into the active channel will lower the average E_{Be}/E_{Al} ratio of fluvial sediment during transport (Wittmann et al., 2009; Fig. 1). Geomorphic processes responsible for sediment reworking in transfer zones vary widely depending on basin morphology, tectonics, and climatology. Extensive sediment storage followed by remobilization is documented in meandering, low-lying, tropical river systems that are eroding old floodplains (Wittmann et al., 2011), arid river systems that source sediment from sand dunes containing long-buried sediments (Eccleshall, 2019; Vermeesch et al., 2010), and hydrologically-variable basins where flood events remobilize vertically-accreted floodplain deposits (Codilean et al., 2021). While old, deeply-buried deposits typically have low nuclide concentrations and thus less influence on the average E_{Be}/E_{Al} ratio when mixed with active channel sediment in small amounts, high flow events may re-mobilize substantial volumes of old, buried sediment and have a significant impact on nuclide concentrations (e.g., Codilean et al. 2021; Wittmann et al., 2011) and calculated E_{Be}/E_{Al} ratios.

3 Methods

3.1 Study Design – Approach and Limitations

In this study, we use a compilation of previously-published (n = 503) and new (n = 121) paired ^{10}Be and ^{26}Al concentration measurements in fluvial sediments to test for storage and remobilization during sediment generation and/or transport. We calculate nuclide-specific erosion rates and use the agreement or discordance between these rates to identify burial during transport. We measure the morphometric and climatological properties of basins from which the sampled sediments derive and use a variety of statistical analyses to assess if basin properties are correlated with cosmogenic indications of such burial. Then, we consider geomorphic mechanisms to explain observed correlations and discuss the implications of our results for the widely-used basin-averaged ^{10}Be erosion rate method.

Measured ^{26}Al and ^{10}Be alone cannot provide sediment storage durations or identify specific geomorphic histories for each sample because sediment samples are mixtures of grains with different histories and the inverse solutions are non-unique (Bierman and Steig, 1996; von Blanckenburg, 2005; Brown et al., 1995; Granger et al., 1996; Schaefer et al., 2022). The rate of E_{Be}/E_{Al} lowering in stored sediment is depth-dependent (Wittmann and von Blanckenburg, 2009). Thus, the mixing of grains with different storage depth and time histories, and consequently varying histories and duration of nuclide decay and production, precludes accurate estimations of storage duration. Although we identify basin properties that correlate with isotopic indications of burial and storage, the identification of specific processes responsible for storage and subsequent remobilization likely differs on a case-by-case basis.

https://doi.org/10.5194/gchron-2024-22
Preprint. Discussion started: 28 August 2024

3.2 Data sources

We used two data sources: measurements in reported published studies (n = 503) and ^{26}Al and ^{10}Be concentrations from new ^{26}Al measurements made on samples archived at the University of Vermont (UVM) that had previously published ^{10}Be concentrations (n = 121). For all samples, we normalized originally-reported ^{10}Be concentrations to the 07KNSTD standard (Nishiizumi et al., 2007) and ^{26}Al concentrations to the KNSTD standard (Nishiizumi, 2004) using conversion factors based on the original AMS standards used for normalization (Balco et al., 2008; Nishiizumi et al., 2007).

3.2.1 Sources of previously published paired ^{26}Al and ^{10}Be measurements

We sourced data from the OCTOPUS database (Codilean et al., 2018; Codilean et al., 2022) for previously-published paired ^{26}Al and ^{10}Be measurements from fluvial sediments around the world with robust documentation of processing methods, including the Al and Be standards used during AMS measurements (n = 431). We also compiled samples from recently-published studies that have not yet been added to the OCTOPUS database (n = 72; Wang et al., 2017; Adams and Ehlers, 2018; Mason and Romans, 2018; Moon et al., 2018; Hattanji et al., 2019; Hubert-Ferrari et al., 2021; Yang et al., 2021; Zhang et al., 2021; Ben-Israel et al., 2022; Zhang et al., 2022). Previously-published samples were processed at numerous laboratories, including at UVM, and were analyzed at several AMS facilities (sources, raw data, and AMS facilities for previously published samples are reported in Table S1).

3.2.2 Sample processing for new ^{26}Al measurements

Samples with new ^{26}Al measurements come from a wide range of locations but were processed entirely at UVM. These archived samples had previously undergone Be and Al extraction following established methods (Corbett et al., 2016) but only had ^{10}Be concentrations measured (^{10}Be concentration measurements were originally reported in their source publications and are provided in Table S2). The Al-bearing fraction of these archived samples, Al and Be having been separated by column chromatography during the original sample processing for ^{10}Be analysis (Corbett et al., 2016), were stored as Al hydroxide gels.

We re-dissolved the gels into a chloride liquid form using 1 mL of 6 mol/L hydrochloric acid and allowed the gels to sit in acid for several weeks. When completely dissolved, we added 4 mL of water to each sample to create a 1.2 mol/L hydrochloric acid solution for column chromatography and centrifuged the samples to remove any lingering undissolved material. We removed ^{26}Mg, an isobar of ^{26}Al, via column chromatography and then followed the methods outlined in Corbett et al. (2016) to convert samples into an Al oxide powder mixed with Nb for ^{26}Al/^{27}Al measurement via accelerator mass spectrometry (AMS).

^{26}Al/^{27}Al ratios for these re-processed samples were measured using AMS between 2019 and 2021 at the Purdue Rare Isotopes Measurement Laboratory (PRIME), where the addition of a gas-filled magnet to the AMS has significantly reduced ^{26}Al measurement uncertainties (Caffee et al., 2015). Samples were measured against primary standard KNSTD with a ^{26}Al/^{27}Al ratio of 1.818 x 10^{-12} (Nishiizumi, 2004). We re-processed blanks that were archived with the Al hydroxide gels from their original processing batches (n = 37) and blank-corrected samples by subtracting the average $^{26}Al/^{27}Al$ ratio from all re-processed blanks (2.56 +/- 2.20 x 10^{-15}; 1SD, all blank measurements and calculations can be found in Table S2). We propagated AMS $^{26}Al/^{27}Al$ and blank measurement uncertainties in quadrature to quantify total ^{26}Al concentration uncertainty. All new ^{26}Al concentration measurements and calculations are reported in Table S2.

3.3 Calculating ^{10}Be and ^{26}Al-derived erosion rates and erosion rate discordance

We use the erosion rate calculator formerly known as CRONUS v3 (Balco et al., 2008) with the nuclide-specific LSDn scaling scheme (Lifton et al., 2014) to calculate erosion rates separately for ^{10}Be (E_{Be}) and ^{26}Al (E_{Al}). We used mean basin elevations for E_{Be} and E_{Al} calculations and assumed no shielding; these approximations are reflected in both erosion rate calculations and therefore should not introduce biases in our analysis. We propagated 'external' uncertainties (i.e., incorporating analytical and production rate uncertainties) of E_{Be} and E_{Al} estimates in quadrature to quantify the 1-sigma (1σ) uncertainty of E_{Be}/E_{Al}.

An E_{Be}/E_{Al} value of 1 (within uncertainty) is consistent with a history without burial (but does not necessarily preclude burial and then re-exposure). An E_{Be}/E_{Al} less than 1 (considering uncertainty) is consistent with a history including burial and remobilization of sediment back into the active channel.

3.4 Quantifying basin parameters

For each basin, we calculated ^{10}Be and ^{26}Al-derived erosion rates, mean basin slope, basin area, local relief using a 2 km radius circular moving window, mean annual precipitation, aridity, tectonic activity, dominant lithology, and likelihood of stream flow intermittence (data sources and detailed methods are reported in the Supplementary Material). We created basins shapefiles by delineating watersheds upstream of sediment sampling locations (following the procedures used in the OCTOPUS database; Codilean et al., 2022) and used these shapefiles to calculate zonal statistics within each basin. We determined all sampling locations from the source publications or through personal correspondence with the papers' authors. We treated nested basins individually, such that a sample collected in an upstream tributary basin has a separate basin shapefile from the larger, downstream sample with a basin encompassing all upstream tributaries.

3.5 Statistical analyses

We used hypothesis testing methods to determine if physical or climatological characteristics of sample basins correlate significantly with calculated E_{Be}/E_{Al} values. We used correlation analyses between E_{Be}/E_{Al} values and numerical basin parameters (latitude, mean erosion rate, area, mean area, mean slope, mean local relief, annual precipitation, aridity index, and intermittent flow probability) and checked for cross-correlation between all basin parameters. We log-transformed basin areas and basin-averaged ^{10}Be erosion rates prior to correlation analyses to normalize their skewed distribution (Fig. 4) and used the non-parametric Spearman's Correlation Coefficient to evaluate the strength of correlations due to the lingering non-normality of some basin parameter distributions. We used a forward stepwise regression analysis as in Portenga and Bierman (2011) to create a multi-variate linear model relating E_{Be}/E_{Al} values to basin parameters. This analysis considers all basin parameters but only fits a regression

https://doi.org/10.5194/gchron-2024-22
Preprint. Discussion started: 28 August 2024

through those that are most statistically important as defined by the change in p-value of the model F-statistic when adding or removing each parameter. We set the probability to enter as $p < 0.05$ and the probability to leave as $p > 0.1$.

We use one-way analysis of variance (ANOVA) and Tukey multiple comparison of means testing (Abdi and Williams, 2010) to assess the magnitude and statistical significance of E_{Be}/E_{Al} value differences between categorical variables (tectonic activity, dominant lithology, region) and to identify threshold values for E_{Be}/E_{Al} differences based on basin areas. We ran the same analyses using the Kruskal-Wallis H test for multiple comparison of medians (MacFarland and Yates, 2016) and obtained nearly identical results to the Tukey MCM testing; we report only the mean results. We used the python libraries *pandas*, *matplotlib*, *cartopy*, *numpy*, *seaborn*, *scipy*, and *statsmodels* to perform all statistical analyses (except for the forward stepwise regression analysis) and create figures, and a Jupyter notebook with coding for all analyses (including the median analyses) is included in the Supplementary Material. We used MATLAB to perform the forward stepwise regression analysis using the '*stepwiselm*' function; a copy of this script can be found in the Supplementary Material.

4 Results

4.1 Dataset statistics

The compilation of basins assembled here (n = 624) has near-global coverage, although there are fewer data from low-latitude regions, especially at high elevations (Figs 2 and 3). Most basins are < 100,000 km^2 (n = 550), while a small number (n = 25) are very large (>1,000,000 km^2; Fig 2). The basins in the compilation encompass a wide range of morphologic and climatic regimes (Fig 4). The distributions of most basin parameters are right-skewed, with the majority of basins having low-to-moderate slope, relief, and precipitation. The basins are underlain by a variety of dominant lithologies and are split about evenly between those that are tectonically active (n = 339) and those that are post-orogenic (n = 285).

https://doi.org/10.5194/gchron-2024-22
Preprint. Discussion started: 28 August 2024

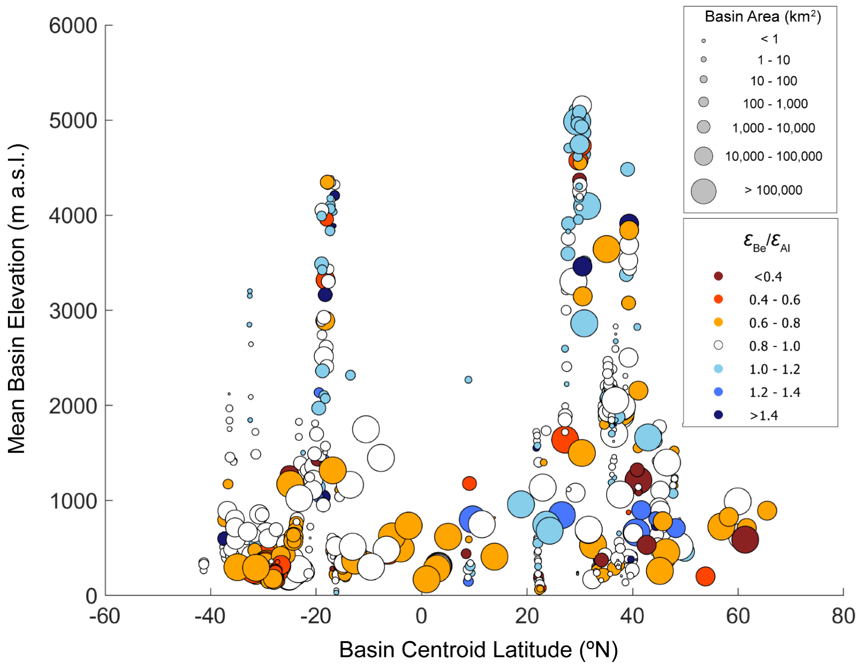

Figure 2. Latitude and elevation distribution of basins in our compilation. Color coding indicates calculated E_{Be}/E_{Al} values while circle size indicates basin area.

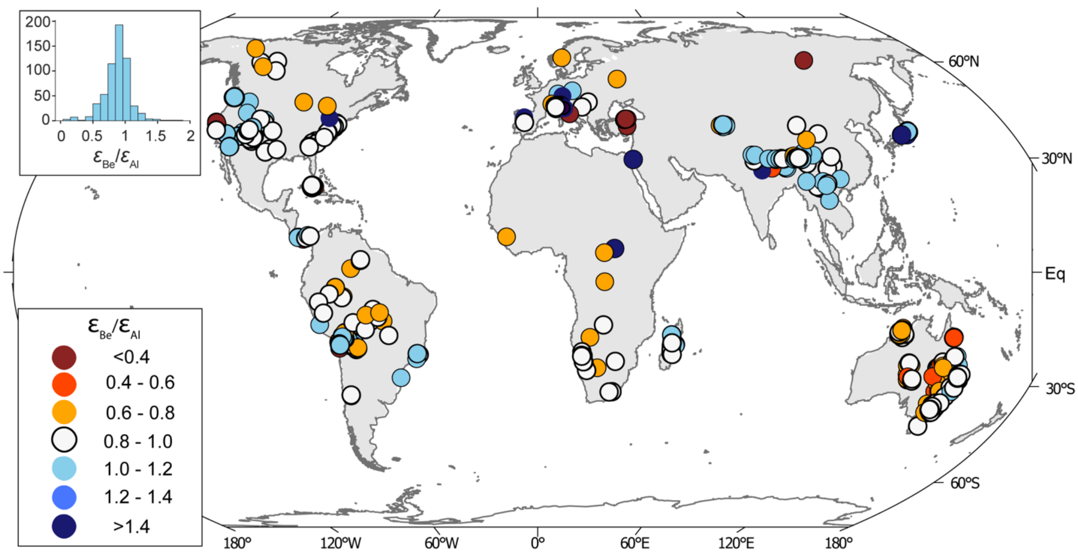

Figure 3. Inset: Distribution of E_{Be}/E_{Al} values. Main: Map of basin centroid locations color-coded by E_{Be}/E_{Al} values.

https://doi.org/10.5194/gchron-2024-22
Preprint. Discussion started: 28 August 2024

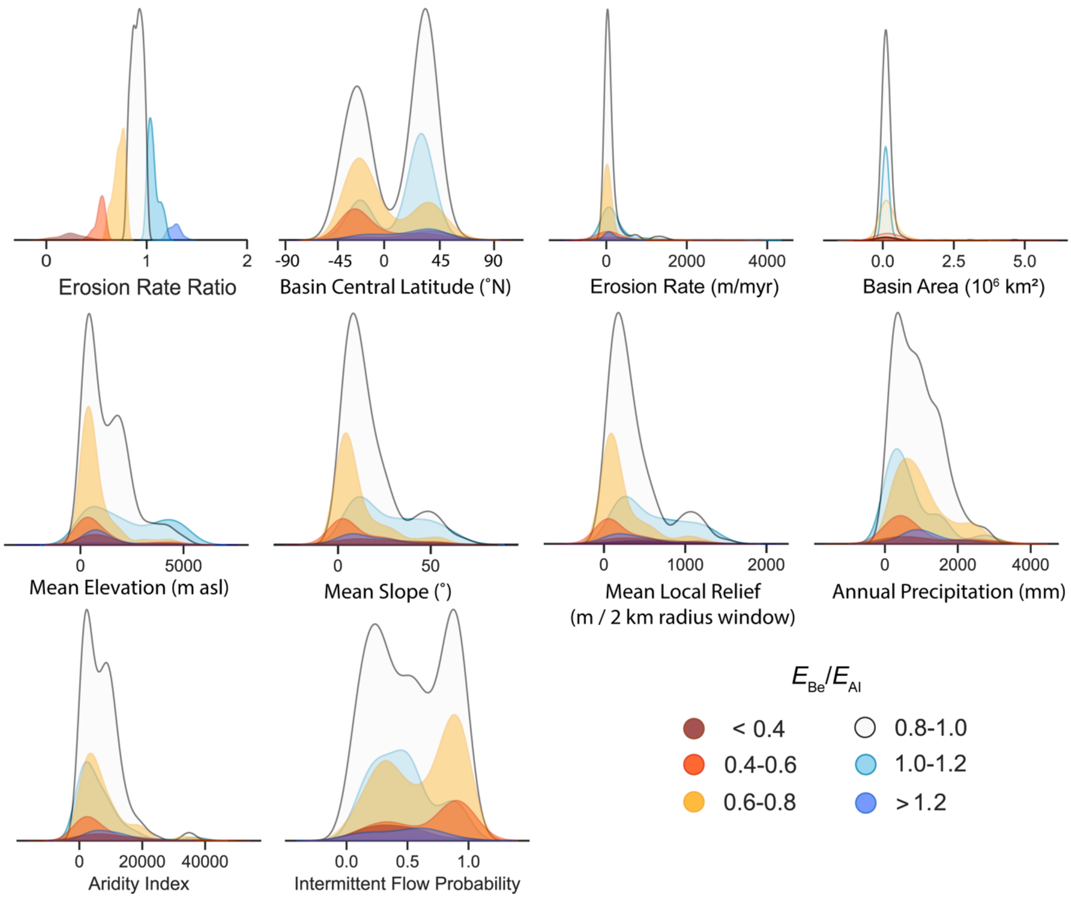

Figure 4. Kernel density distributions of basin parameters with subdivision and color-coding based on E_{Be}/E_{Al} values (see legend). Note that the erosion rate and basin area plots contain data to both x-axis limits. Vertical axes on all plots are relative density values. Sources for all parameters and methods used in their calculations are provided in the Supplementary Materials.

The population of E_{Be}/E_{Al} values (n = 624) approximates a normal distribution with mean = 0.88 and SD = 0.21 (Fig 4 inset). Approximately 44% of the samples in the compilation (n = 276) have E_{Be}/E_{Al} values that do not overlap with 1 when considering 1σ uncertainties; this drops to approximately 14% of samples (n = 87) when considering 2σ uncertainties.

4.2 Correlation analysis and stepwise regression

Of the basin parameters, all but aridity index exhibit statistically-significant correlations with E_{Be}/E_{Al} values ($p < 0.05$), although none of the correlations are particularly strong ($r_s < 0.4$; Figure 5).

https://doi.org/10.5194/gchron-2024-22
Preprint. Discussion started: 28 August 2024

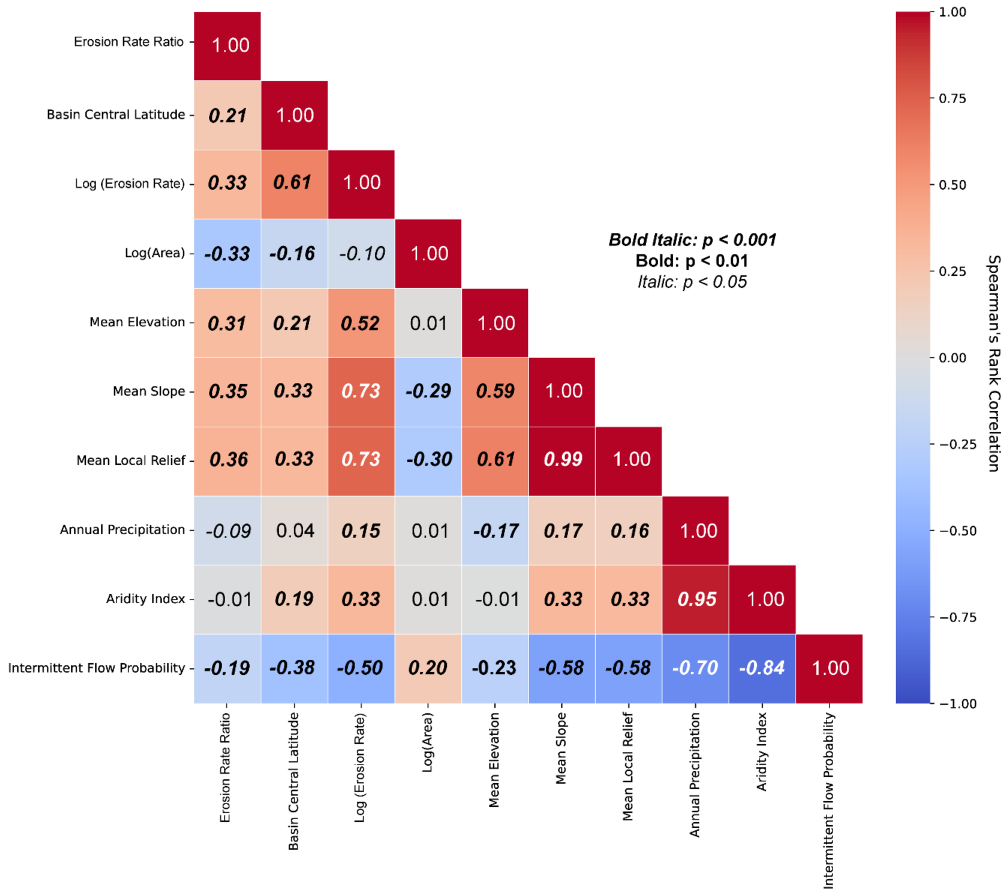

Figure 5. Cross-correlation matrix for basin parameters and E_{Be}/E_{Al} values. Color scale shows Spearman's Correlation Coefficient values and font styling indicates statistical significance (p value) of correlation coefficient.

The best-fitting linear model from the forward stepwise regression analysis (Table 1) predicts a decrease in E_{Be}/E_{Al} values with increasing basin area, decreasing basin-averaged erosion rate, decreasing basin mean elevation, and decreasing basin mean slope. No other basin parameters improved this bi-variate model and thus were removed during the stepwise regression analysis. This model represents a statistically-significant improvement over a constant model ($p << 0.001$), although a low reduced chi-squared statistic (0.042) suggests that it may overfit the data.

https://doi.org/10.5194/gchron-2024-22
Preprint. Discussion started: 28 August 2024

Table 1: Summary of linear model (E_{Be}/E_{Al} ~ β + X + Y) output from forward stepwise regression analysis

	Estimate	SE	tStat	p-value
(Intercept)	0.838	0.022	38.256	3.196e-165
Log(Area)	-0.015	0.002	-7.378	5.200e-13
Log(Erosion Rate)	0.043	0.007	6.329	4.753e-10
Mean Elevation	3.453e-05	7.342e-06	4.704	3.154e-06
Mean Slope	0.003	8.026e-04	3.896	1.085e-04

Number of observations: 624, Error degrees of freedom: 619
Root Mean Squared Error: 0.192, R-squared: 0.177, Adjusted R-Squared: 0.172
F-statistic vs. constant model: 33.3, p-value = 3.41e-25
Reduced Chi-Square: 0.042

4.3 ANOVA testing

ANOVA testing offers more granular insight into the decline of E_{Be}/E_{Al} values with increasing basin area, and among categorical basin parameters suggests that tectonic activity, but not dominant lithology, has a significant correlation with measured E_{Be}/E_{Al} values (Figure 6). Post-hoc tests using group mean and median values produced nearly identical results; mean tests are shown here while the results from median post-hoc tests are included in the supplementary information.

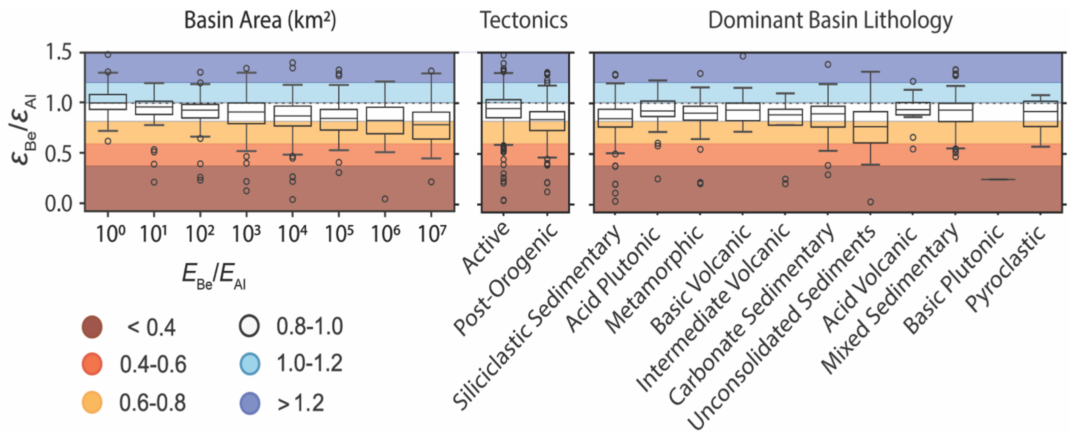

Figure 6. One-way ANOVA results comparing E_{Be}/E_{Al} values between basin area categories (left, basins in each category have areas less than or equal to the label on the x-axis), basin tectonic activity (center), and dominant basin lithology (right). In each plot, boxes show median (center line), 25th and 75th percentile values (box edges) and the maximum and minimum non-outlier values (whiskers). E_{Be}/E_{Al} values plotted as circles are considered outliers. The dashed horizontal line in all plots is a reference line for E_{Be}/E_{Al} = 1. Note that n=6 samples have E_{Be}/E_{Al} > 1.5 and are cropped out of this figure.

With basin areas binned on a logarithmic base-10 scale, a decline in E_{Be}/E_{Al} values with increasing basin area is clear (Figure 6; Table 2). Very small basins (≤1 km^2) have a mean E_{Be}/E_{Al} value of approximately 1 (μ = 1.019 ± 0.155, n = 46) while the largest basins (>1,000,000 km^2) have a mean E_{Be}/E_{Al} value of 0.787 ± 0.253 (n = 25). We

https://doi.org/10.5194/gchron-2024-22
Preprint. Discussion started: 28 August 2024

compare mean E_{Be}/E_{Al} values of other basin area categories against the very small basins and find that basins larger than 10^3 km^2 have mean measured E_{Be}/E_{Al} values lower than 1 ($p < 0.01$). The percentage of basins with E_{Be}/E_{Al} values that overlap with 1 (considering 1σ uncertainties) increases from <9% in the < 1 km^2 area bin to 50% in the 10^4 km^2 area bin and remains around 50% for all larger basins (Table 2).

Table 2: One-way ANOVA results comparing measured E_{Be}/E_{Al} values between basin area categories. Note that the label for each basin area category shows the upper limit for basin areas in that bin.

Basin Area (km²)	**n**	**E_{Be}/E_{Al} Mean**	**E_{Be}/E_{Al} S.D.**	**MCMean to 10^0 km² basins, p-value***	**% of Basins with E_{Be}/E_{Al} < 1****
10^0	41	1.02	0.14	-	7
10^1	56	0.93	0.17	0.39	16
10^2	101	0.92	0.18	0.13	30
10^3	134	0.89	0.23	0.02	39
10^4	122	0.85	0.22	<0.01	51
10^5	82	0.84	0.20	<0.01	56
10^6	63	0.81	0.20	<0.01	48
10^7	25	0.79	0.25	<0.01	52

**Shows p-value for Tukey multi-comparison of means test performed between basin area category and the smallest basins (<10^0 km^2)*

***Including 1σ uncertainties*

We find that basins in tectonically active settings have higher E_{Be}/E_{Al} values ($\mu = 0.93 \pm 0.22$, $n = 339$) than post-orogenic basins ($\mu = 0.81 \pm 0.18$, $n = 285$); this difference is statistically significant ($p << 0.01$). Meanwhile, dominant basin lithology has less of an influence on E_{Be}/E_{Al} values (Fig 6, Table 3). Most lithologies have mean E_{Be}/E_{Al} values that are statistically indistinguishable from each other. There are several exceptions; basins composed primarily of unconsolidated sediments have, on average, lower E_{Be}/E_{Al} values than other lithologies ($\mu = 0.78 \pm 0.23$, $n = 103$, $p < 0.01$), while siliciclastic sedimentary rocks ($\mu = 0.85 \pm 0.17$, $n = 186$) have lower E_{Be}/E_{Al} values than mixed sedimentary ($\mu = 0.93 \pm 0.21$, $n = 96$, $p = 0.03$) and acid plutonic ($\mu = 0.95 \pm 0.14$, $n = 82$, $p = 0.02$) rocks.

https://doi.org/10.5194/gchron-2024-22
Preprint. Discussion started: 28 August 2024

Table 3: Mean E_{Be}/E_{Al} values and standard deviations for dominant basin lithologies as defined in the GLiM database (Hartmann and Moosdorf, 2012)

Lithology	n	E_{Be}/E_{Al} Mean	E_{Be}/E_{Al} S.D.
Acid Plutonic	82	0.95	0.14
Acid Volcanic	28	0.95	0.13
Basic Volcanic	13	0.95	0.20
Carbonate Sedimentary	26	0.95	0.41
Intermediate Volcanic	9	0.78	0.32
Metamorphic	76	0.89	0.18
Mixed Sedimentary	96	0.93	0.21
Pyroclastic	4	0.88	0.22
Siliciclastic Sedimentary	186	0.85	0.17
Unconsolidated Sediments	103	0.78	0.23

5 Discussion and implications

5.1 Prevalence and potential mechanisms causing complex sediment histories

We find widespread evidence of sediment histories that likely include extended sediment storage on timescales of 10^5 – 10^6 years as indicated by E_{Be}/E_{Al} values < 1 (considering 1σ uncertainties) in nearly half of basins (n = 281). The occurrence and magnitude of depressed E_{Be}/E_{Al} values is correlated with several basin morphological parameters, suggesting a systematic and thus predictable relationship between basin morphology and sediment history. Although most physical basin parameters exhibited statistically significant correlations with measured E_{Be}/E_{Al} values (Fig. 2), widespread cross-correlations exist between these parameters and suggest several basin characteristics are more likely to result sediment histories including extended burial.

The stepwise linear regression and ANOVA testing suggests that basin area has the single largest influence on E_{Be}/E_{Al} values (Figs 5 and 6, Tables 1 and 2). The influence of basin area is apparent in the southern Appalachian mountains of the United States (Reusser et al., 2015; Table 4), where large (>1,000 km^2, n = 5) basins have a lower average E_{Be}/E_{Al} value (0.81 ± 0.05) than small basins (<30 km^2, n = 7, E_{Be}/E_{Al} = 0.91 ± 0.06, p = 0.017), despite other physical basin parameters being similar.

Other physical basin parameters play secondary and interlinked roles in determining erosion rate discordance (Fig 5, Table 1). Mean basin slope and elevation are positively correlated with each other and with E_{Be}/E_{Al} values, suggesting that alpine basins—which are typically steeper than lowland basins—produce fluvial sediment that has experienced minimal storage and burial. Similarly, basin-averaged erosion rates and intermittent river flow probability exhibit significant correlations with E_{Be}/E_{Al} values and are negatively correlated to each other, suggesting that slowly-

https://doi.org/10.5194/gchron-2024-22
Preprint. Discussion started: 28 August 2024

eroding basins that regularly experience intermittent river flow are conducive to sediment burial. The influence of basin slope, elevation, and tectonic activity is observed when comparing basins of similar areas in high-alpine Bhutan (Portenga et al., 2015) and low-lying eastern Australia (Codilean et al., 2021); the Bhutan basins have E_{Be}/E_{Al} values near 1 (0.98 ± 0.06, n = 11) while eastern Australian basins have lower average E_{Be}/E_{Al} values (0.83 ± 0.06, n = 7, $p < 0.001$) indicating extensive sediment storage (Table 4).

Based on cross-correlations between physical basin parameters, we distill our findings into two general categories. Sediment sourced from large lowland basins— particularly those over 1,000 km^2, with low average erosion rates, low mean slopes, and in post-orogenic settings— is more likely to exhibit erosion rate discordance indicative of sediment storage and burial in source and/or transfer zones. Smaller alpine basins, particularly steeper basins with higher average erosion rates in tectonically active regions, are more likely to produce sediment with E_{Be}/E_{Al} values that overlap with 1 (within 1 standard deviation analytical uncertainties), suggesting minimal sediment storage (<10^5 years). We infer that this is because larger, more gently sloping basins in tectonically quiescent regions offer more opportunities for extended, stable sediment storage in floodplains.

Table 4: E_{Be}/E_{Al} regional case studies

Location	n	E_{Be}/E_{Al} mean	E_{Be}/E_{Al} S.D.	Mean basin elevation (m a.s.l.)	Mean basin slope (°)	Mean basin area (km^2)
Southern Appalachians, USA (small basins; Reusser et al., 2015)	7	0.91	0.06	337	5.5	9
*Southern Appalachians, USA (large basins; Reusser et al., 2015)**	5	0.81	0.05	281	7	6262
*Bhutan alpine basins (Portenga et al., 2015)***	11	0.98	0.08	3373	49.4	164
Lockyer sub-basins, Eastern Australia (Codilean et al., 2021)	7	0.83	0.06	430	15.5	130

**One outlier with E_{Be}/E_{Al} = 0.22 was removed. The low ratio of this sample was attributed to laboratory error in the source publication.*

***For this comparison we removed basins larger than 1000 km^2 (n = 3)*

Climatological variables appear to play only a minor role in the occurrence and magnitude of erosion rate discordance. We found very weak correlations between E_{Be}/E_{Al}, mean annual precipitation, and aridity (Fig 5; Table 1). However, intermittent flow probability exhibited a significant negative correlation to E_{Be}/E_{Al} values (Fig 5), suggesting that basins with a higher probability of discontinuous flow for at least one day per year are more likely to contain sediment with an extended history of burial. While fluvial systems that experience intermittent flow are most common in arid and semiarid regions (Costigan et al., 2017), they are prevalent around the world and intermittent flow probability is correlated with a variety of hydrologic, geologic, and morphologic variables in addition to climate regime (Messager et al., 2021; Figure 6). Therefore, we cannot confidently attribute an exclusively climatological root for the correlation between intermittent flow probability and isotopic evidence of sediment burial.

https://doi.org/10.5194/gchron-2024-22
Preprint. Discussion started: 28 August 2024

Some low E_{Be}/E_{Al} values, and values greater than 1, in this compilation are likely due to laboratory biases that influence measured nuclide concentrations. Critical to the accuracy of ^{26}Al and ^{10}Be measurements by AMS is the quantification of total aluminum and beryllium in samples (the stable isotopes, ^{27}Al and ^{9}Be which are many orders of magnitude greater in concentration that the radionuclides ^{26}Al and ^{10}Be). Stable beryllium at detectable levels in quartz is rare but occasionally present (e.g., Portenga et al., 2015), and not all laboratories quantify total Be in samples. Unaccounted-for native ^{9}Be will lower measured ^{10}Be/^{9}Be ratios, lower calculated ^{10}Be concentrations, and increase calculated ^{26}Al/^{10}Be ratios. Conversely, stable aluminum (^{27}Al) is ubiquitous in quartz, meaning that full retention and accurate measurement of that isotope, typically via inductively coupled plasma optical emission spectroscopy after quartz dissolution (ICP-OES; e.g., Corbett et al., 2016), is critical to properly quantifying the concentration of ^{26}Al. Low recovery of total Al before ICP-OES results in lower than actual ^{26}Al/^{10}Be ratios (Bierman and Caffee, 2002; Corbett et al., 2016). Finally, incomplete removal of meteoric ^{10}Be during quartz purification can also increase calculated in situ ^{10}Be concentrations, thus lowering ^{26}Al/^{10}Be ratios (Corbett et al., 2022). While some scatter in the data is likely the result of such laboratory errors, the observed systematic correlations between morphological basin parameters and E_{Be}/E_{Al} values suggests that most low ratios are due to geologic, rather than laboratory, processes.

5.2 Implications for cosmogenically-derived erosion rates and understanding landscapes

This analysis shows that nearly half of all samples for which multi-nuclide measurements exist have discordance between erosion rates derived from ^{10}Be and ^{26}Al beyond 1σ uncertainty. Although some discordant samples may be the result of laboratory errors (most likely inadvertent underestimation of stable ^{27}Al and incorporation of meteoric ^{10}Be in quartz), many represent the complex history of sediment in drainage basins. Because our regression analysis shows that large, low-slope, low-erosion-rate basins are most likely to have sediment with discordant ^{10}Be and ^{26}Al-derived erosion rates, such complexity is most likely the result of extended sediment storage (>10^5 years) in low gradient floodplains typical of such basins – sufficient time for decay of ^{26}Al to be reliably measurable.

The impact of sediment storage on the veracity of cosmogenically-determined erosion rates is difficult to assess for several reasons. First, sediment samples are a mixture of material, meaning that every sample contains many thousands of sand grains each of which has its own idiosyncratic history. Such mixing means that any attempt at decay correction will be flawed as mixing is a linear process and decay correction is not. Second, sediment both loses nuclides (through radio decay) and gains nuclides (by production at depth) while in storage. The resulting nuclide concentration is a convolution of time and depth in storage where depth is almost certainly not constant over time. Finally, lowering of sediment E_{Be}/E_{Al} ratios is due to the outpacing of ^{26}Al decay compared to ^{10}Be, which behaves more like a stable isotope on timescales between 10^5 – 10^6 years. Thus, a low E_{Be}/E_{Al} ratio may suggest sediment storage on these timescales but need not imply that ^{10}Be-derived erosion rates are biased significantly by ^{10}Be decay.

Perhaps it is more useful to consider the E_{Be}/E_{Al} ratio in sediment samples as a window into watershed processes. With field and remote sensing data, it is possible to estimate volumes of sediment in storage on lowland floodplains (Dunne et al., 1998). Sampling of depth profiles along cut banks and in drill cores can provide quantification of nuclide concentrations in material stored in the floodplain (Bierman et al., 2005). Measuring cosmogenic nuclides in samples collected down drainage networks can demonstrate if nuclide activities and ^{26}Al/^{10}Be ratios change with basin area

https://doi.org/10.5194/gchron-2024-22
Preprint. Discussion started: 28 August 2024

and average slope (Clapp et al., 2002; Reusser et al., 2017). Together, these data can elucidate landscape behavior at a variety of scales and bring a deeper understanding of sediment routing and erosion rates throughout large drainage basis.

6 Conclusions

The discordance between basin-averaged erosion rates derived from in situ cosmogenic ^{10}Be and ^{26}Al in detrital fluvial samples provides insights into geomorphic controls on sediment routing dynamics. We calculated the ratio between ^{10}Be and ^{26}Al-derived erosion rates (E_{Be}/E_{Al}) in a global compilation of detrital fluvial samples with measurements from both nuclides (n = 624, of which n = 121 are new) and found that nearly half of samples (n = 276) exhibit erosion rate discordance as indicated by $E_{Be}/E_{Al} < 1$ (considering 1σ uncertainties). Low E_{Be}/E_{Al} values in detrital sediments are most likely the result of ^{26}Al decay during extended storage (>10^5 years) on hillslopes or in fluvial networks. Source basin area appears to have the greatest influence on sediment E_{Be}/E_{Al} values, with basins >1,000 km^2 producing sediment that, on average, has E_{Be}/E_{Al} values significantly less than 1. Other physical basin parameters have secondary and interlinked correlations to E_{Be}/E_{Al} values, allowing us to separate basins into two general categories. Large, low-slope, lowland basins in post-orogenic settings are more likely to produce sediment exhibiting erosion rate discordance indicative of extended sediment storage (>10^5 years). Smaller (<1,000 km^2), steep, alpine basins in tectonically active settings are more likely to produce sediment exhibiting erosion rate agreement indicative of minimal sediment storage (<10^5 years). These results provide global-scale insights into sediment routing system dynamics and demonstrate the utility of a multi-nuclide approach for understanding geomorphic processes at the scale of drainage basins.

https://doi.org/10.5194/gchron-2024-22
Preprint. Discussion started: 28 August 2024

Code and Data Availability

The supplementary information for this study, including supplementary data tables, text, and a Jupyter Notebook and Matlab script containing code for the statistical analyses and figure production, are available on a public Github repository that can be found with DOI: 10.5281/zenodo.13345369

Author Contributions

PB and LC conceptualized the study and acquired funding while CH conducted the investigation. PB and LC provided laboratory resources for cosmogenic nuclide chemical processing and LC supervised CH while he performed the chemistry procedures. MC performed the measurement of cosmogenic nuclide ratio measurements via AMS and assisted with interpretation of results. CH and AC were responsible for compiling previously published nuclide measurement and performing geospatial analyses, while CH performed the statistical analyses. CH prepared all data visualizations and prepared the original manuscript draft. CH, PB, LC, AC, and MC worked together to review and edit manuscript drafts, and all agreed on the final draft for journal submission.

Competing Interests

The authors declare that they have no conflict of interest.

https://doi.org/10.5194/gchron-2024-22
Preprint. Discussion started: 28 August 2024

References

Abdi, H. and Williams, L. J.: Tukey's Honestly Significant Difference (HSD) Test, in: Encyclopedia of Research Design, Sage, Thousand Oaks, CA, 2010.

Allen, P. A.: Time scales of tectonic landscapes and their sediment routing systems, Geological Society, London, Special Publications, 296, 7–28, 2008.

Allen, P. A.: Sediment Routing Systems: The Fate of Sediment from Source to Sink, Cambridge University Press, Cambridge, https://doi.org/10.1017/9781316135754, 2017.

Balco, G. and Rovey, C. W.: An isochron method for cosmogenic-nuclide dating of buried soils and sediments, American Journal of Science, 308, 1083–1114, https://doi.org/10.2475/10.2008.02, 2008.

Balco, G., Stone, J. O., Lifton, N. A., and Dunai, T. J.: A complete and easily accessible means of calculating surface exposure ages or erosion rates from 10Be and 26Al measurements, Quaternary Geochronology, 3, 174–195, https://doi.org/10.1016/j.quageo.2007.12.001, 2008.

Ben-Israel, M., Armon, M., Team, A., and Matmon, A.: Sediment residence times in large rivers quantified using a cosmogenic nuclides based transport model and implications for buffering of continental erosion signals, Journal of Geophysical Research: Earth Surface, 127, e2021JF006417, 2022.

Bierman, P. and Caffee, M.: Cosmogenic exposure and erosion history of Australian bedrock landforms, Geological Society of America Bulletin, 114, 787–803, https://doi.org/10.1130/0016-7606(2002)114, 2002.

Bierman, P. and Steig, E. J.: Estimating rates of denudation using cosmogenic isotope abundances in sediment, Earth Surface Processes and Landforms, 21, 125–139, https://doi.org/10.1002/(SICI)1096-9837(199602)21:2<125::AID-ESP511>3.0.CO;2-8, 1996.

Bierman, P., Clapp, E., Nichols, K., Gillespie, A., and Caffee, M. W.: Using cosmogenic nuclide measurements in sediments to understand background rates of erosion and sediment transport, in: Landscape Erosion and Evolution Modeling, Springer, 89–115, 2001.

Bierman, P. R. and Caffee, M.: Slow Rates of Rock Surface Erosion and Sediment Production Across the Namib Desert and Escarpment, Southern Africa, American Journal of Science, 301, 326–358, https://doi.org/10.2475/ajs.301.4-5.326, 2001.

Bierman, P. R. and Nichols, K. K.: Rock to sediment—slope to sea with 10Be—rates of landscape change, Annu. Rev. Earth Planet. Sci., 32, 215–255, 2004.

Bierman, P. R., Reuter, J. M., Pavich, M., Gellis, A. C., Caffee, M. W., and Larsen, J.: Using cosmogenic nuclides to contrast rates of erosion and sediment yield in a semi-arid, arroyo-dominated landscape, Rio Puerco Basin, New Mexico, Earth Surface Processes and Landforms, 30, 935–953, https://doi.org/10.1002/esp.1255, 2005.

von Blanckenburg, F.: The control mechanisms of erosion and weathering at basin scale from cosmogenic nuclides in river sediment, Earth and Planetary Science Letters, 237, 462–479, https://doi.org/10.1016/j.epsl.2005.06.030, 2005.

Blöthe, J. H. and Korup, O.: Millennial lag times in the Himalayan sediment routing system, Earth and Planetary Science Letters, 382, 38–46, 2013.

Brown, E. T., Stallard, R. F., Larsen, M. C., Raisbeck, G. M., and Yiou, F.: Denudation rates determined from the accumulation of in situ-produced 10Be in the Luquillo Experimental Forest, Puerto Rico, Earth and Planetary Science Letters, 129, 193–202, 1995.

Campbell, M. K., Bierman, P. R., Schmidt, A. H., Sibello Hernández, R., García-Moya, A., Corbett, L. B., Hidy, A. J., Cartas Águila, H., Guillén Arruebarrena, A., and Balco, G.: Cosmogenic nuclide and solute flux data from central Cuban rivers emphasize the importance of both physical and chemical mass loss from tropical landscapes, Geochronology, 4, 435–453, 2022.

Carretier, S., Guerit, L., Harries, R., Regard, V., Maffre, P., and Bonnet, S.: The distribution of sediment residence times at the foot of mountains and its implications for proxies recorded in sedimentary basins, Earth and Planetary Science Letters, 546, 116448, https://doi.org/10.1016/j.epsl.2020.116448, 2020.

Cazes, G., Fink, D., Codilean, A. T., Fülöp, R., Fujioka, T., and Wilcken, K. M.: 26Al/10Be ratios reveal the source of river sediments in the Kimberley, NW Australia, Earth Surface Processes and Landforms, 45, 424–439, 2020.

Chmeleff, J., Von Blanckenburg, F., Kossert, K., and Jakob, D.: Determination of the 10Be half-life by multicollector ICP-MS and liquid scintillation counting, Nuclear Instruments and Methods in Physics Research Section B: Beam Interactions with Materials and Atoms, 268, 192–199, https://doi.org/10.1016/j.nimb.2009.09.012, 2010.

Clapp, E. M., Bierman, P. R., Schick, A. P., Lekach, J., Enzel, Y., and Caffee, M.: Sediment yield exceeds sediment production in arid region drainage basins, Geology, 28, 995–998, https://doi.org/10.1130/0091-7613(2000)28, 2000.

Clapp, E. M., Bierman, P. R., Nichols, K. K., Pavich, M., and Caffee, M.: Rates of sediment supply to arroyos from upland erosion determined using in situ produced cosmogenic 10Be and 26Al, Quaternary Research, 55, 235–245, https://doi.org/10.1006/qres.2000.2211, 2001.

Clapp, E. M., Bierman, P. R., and Caffee, M.: Using 10Be and 26Al to determine sediment generation rates and identify sediment source areas in an arid region drainage basin, Geomorphology, 45, 89–104, https://doi.org/10.1016/s0169-555x(01)00191-x, 2002.

Codilean, A. T. and Sadler, P. M.: Tectonic Controls on Himalayan Denudation?, AGU Advances, 2, 2021.

Codilean, A. T., Fülöp, R.-H., Munack, H., Wilcken, K. M., Cohen, T. J., Rood, D. H., Fink, D., Bartley, R., Croke, J., and Fifield, L.: Controls on denudation along the East Australian continental margin, Earth-Science Reviews, 214, 103543, 2021.

Codilean, A. T., Munack, H., Saktura, W. M., Cohen, T. J., Jacobs, Z., Ulm, S., Hesse, P. P., Heyman, J., Peters, K. J., Williams, A. N., Saktura, R. B. K., Rui, X., Chishiro-Dennelly, K., and Panta, A.: OCTOPUS database (v.2), Earth Syst. Sci. Data, 14, 3695–3713, https://doi.org/10.5194/essd-14-3695-2022, 2022.

Corbett, L. B., Bierman, P. R., and Rood, D. H.: An approach for optimizing in situ cosmogenic 10Be sample preparation, Quaternary Geochronology, 33, 24–34, https://doi.org/10.1016/j.quageo.2016.02.001, 2016.

Corbett, L. B., Bierman, P. R., Rood, D. H., Caffee, M. W., Lifton, N. A., and Woodruff, T. E.: Cosmogenic 26Al/10Be surface production ratio in Greenland, Geophysical Research Letters, 44, 1350–1359, https://doi.org/10.1002/2016gl071276, 2017.

Corbett, L. B., Bierman, P. R., Brown, T. A., Caffee, M. W., Fink, D., Freeman, S. P. H. T., Hidy, A. J., Rood, D. H., Wilcken, K. M., and Woodruff, T. E.: Clean quartz matters for cosmogenic nuclide analyses: An exploration of the importance of sample purity using the CRONUS-N reference material, Quaternary Geochronology, 73, 101403, https://doi.org/10.1016/j.quageo.2022.101403, 2022.

Dosseto, A., Buss, H. L., and Chabaux, F.: Age and weathering rate of sediments in small catchments: The role of hillslope erosion, Geochimica et Cosmochimica Acta, 132, 238–258, https://doi.org/10.1016/j.gca.2014.02.010, 2014.

Dunne, T., Mertes, L. A. K., Meade, R. H., Richey, J. E., and Forsberg, B. R.: Exchanges of sediment between the flood plain and channel of the Amazon River in Brazil, GSA Bulletin, 110, 450–467, https://doi.org/10.1130/0016-7606(1998)110<0450:EOSBTF>2.3.CO;2, 1998.

Eccleshall, S. V.: The why, when, and where of anabranching rivers in the arid Lake Eyre Basin, Doctor of Philosophy thesis, University of Wollongong, 2019.

Fülöp, R.-H., Codilean, A. T., Wilcken, K. M., Cohen, T. J., Fink, D., Smith, A. M., Yang, B., Levchenko, V. A., Wacker, L., and Marx, S. K.: Million-year lag times in a post-orogenic sediment conveyor, Science Advances, 6, eaaz8845, 2020.

Granger, D. E.: A review of burial dating methods using 26Al and 10Be, in: In Situ-Produced Cosmogenic Nuclides and Quantification of Geological Processes: Geological Society of America Special Paper 415, edited by: Siame, L. L., Bourles, D. L., and Brown, E. T., Geological Society of America, 1–16, https://doi.org/10.1130/2006.2415(01), 2006.

Granger, D. E. and Schaller, M.: Cosmogenic Nuclides and Erosion at the Watershed Scale, Elements, 10, 369–373, https://doi.org/10.2113/gselements.10.5.369, 2014.

Granger, D. E., Kirchner, J. W., and Finkel, R.: Spatially averaged long-term erosion rates measured from in situ-produced cosmogenic nuclides in alluvial sediment, The Journal of Geology, 104, 249–257, https://doi.org/10.1086/629823, 1996.

Hartmann, J. and Moosdorf, N.: The new global lithological map database GLiM: A representation of rock properties at the Earth surface, Geochemistry, Geophysics, Geosystems, 13, https://doi.org/10.1029/2012GC004370, 2012.

Heimsath, A. M., Dietrich, W. E., Nishiizumi, K., and Finkel, R. C.: The soil production function and landscape equilibrium, Nature, 388, 358–361, 1997.

Hidy, A. J., Gosse, J. C., Blum, M. D., and Gibling, M. R.: Glacial–interglacial variation in denudation rates from interior Texas, USA, established with cosmogenic nuclides, Earth and Planetary Science Letters, 390, 209–221, 2014.

Jerolmack, D. J. and Paola, C.: Shredding of environmental signals by sediment transport, Geophysical Research Letters, 37, 2010.

Jonell, T. N., Owen, L. A., Carter, A., Schwenniger, J.-L., and Clift, P. D.: Quantifying episodic erosion and transient storage on the western margin of the Tibetan Plateau, upper Indus River, Quaternary Research, 89, 281–306, https://doi.org/10.1017/qua.2017.92, 2018.

Jungers, M. C., Bierman, P. R., Matmon, A., Nichols, K., Larsen, J., and Finkel, R.: Tracing hillslope sediment production and transport with in situ and meteoric 10Be, Journal of Geophysical Research: Earth Surface, 114, https://doi.org/10.1029/2008JF001086, 2009.

Kober, F., Ivy-Ochs, S., Zeilinger, G., Schlunegger, F., Kubik, P., Baur, H., and Wieler, R.: Complex multiple cosmogenic nuclide concentration and histories in the arid Rio Lluta catchment, northern Chile, Earth Surface Processes and Landforms, 34, 398–412, 2009.

Korschinek, G., Bergmaier, A., Faestermann, T., Gerstmann, U. C., Knie, K., Rugel, G., Wallner, A., Dillmann, I., Dollinger, G., Lierse von Gostomski, C., Kossert, K., Maiti, M., Poutivtsev, M., and Remmert, A.: A new value for the half-life of 10Be

https://doi.org/10.5194/gchron-2024-22
Preprint. Discussion started: 28 August 2024

by Heavy-Ion Elastic Recoil Detection and liquid scintillation counting, Nuclear Instruments and Methods in Physics Research Section B: Beam Interactions with Materials and Atoms, 268, 187–191, https://doi.org/10.1016/j.nimb.2009.09.020, 2010.

Lal, D.: Cosmic ray labeling of erosion surfaces: in situ nuclide production rates and erosion models, Earth and Planetary Science Letters, 104, 424–439, https://doi.org/10.1016/0012-821x(91)90220-c, 1991.

Langbein, W. B. and Leopold, L. B.: Quasi-equilibrium states in channel morphology, American Journal of Science, 262, 782–794, 1964.

Leopold, L. B. and Wolman, M. G.: River meanders, Geological Society of America Bulletin, 71, 769–793, 1960.

Lifton, N., Sato, T., and Dunai, T. J.: Scaling in situ cosmogenic nuclide production rates using analytical approximations to atmospheric cosmic-ray fluxes, Earth and Planetary Science Letters, 386, 149–160, https://doi.org/10.1016/j.epsl.2013.10.052, 2014.

MacFarland, T. W. and Yates, J. M.: Kruskal–Wallis H-Test for Oneway Analysis of Variance (ANOVA) by Ranks, in: Introduction to Nonparametric Statistics for the Biological Sciences Using R, edited by: MacFarland, T. W. and Yates, J. M., Springer International Publishing, Cham, 177–211, https://doi.org/10.1007/978-3-319-30634-6_6, 2016.

Makhubela, T., Kramers, J., Scherler, D., Wittmann, H., Dirks, P., and Winkler, S.: Effects of long soil surface residence times on apparent cosmogenic nuclide denudation rates and burial ages in the Cradle of Humankind, South Africa, Earth Surface Processes and Landforms, 44, 2968–2981, 2019.

Munack, H., Blöthe, J. H., Fülöp, R. H., Codilean, A. T., Fink, D., and Korup, O.: Recycling of Pleistocene valley fills dominates 135 ka of sediment flux, upper Indus River, Quaternary Science Reviews, 149, 122–134, https://doi.org/10.1016/j.quascirev.2016.07.030, 2016.

Nichols, K. K., Bierman, P. R., Hooke, R. L., Clapp, E. M., and Caffee, M.: Quantifying sediment transport on desert piedmonts using 10Be and 26Al, Geomorphology, 45, 105–125, https://doi.org/10.1016/S0169-555X(01)00192-1, 2002.

Nishiizumi, K.: Preparation of 26Al AMS standards, Nuclear Instruments and Methods in Physics Research Section B: Beam Interactions with Materials and Atoms, 223–224, 388–392, https://doi.org/10.1016/j.nimb.2004.04.075, 2004.

Nishiizumi, K., Imamura, M., Caffee, M. W., Southon, J. R., Finkel, R. C., and McAninch, J.: Absolute calibration of 10Be AMS standards, Nuclear Instruments and Methods in Physics Research Section B: Beam Interactions with Materials and Atoms, 258, 403–413, https://doi.org/10.1016/j.nimb.2007.01.297, 2007.

Otto, J., Schrott, L., Jaboyedoff, M., and Dikau, R.: Quantifying sediment storage in a high alpine valley (Turtmanntal, Switzerland), Earth Surface Processes and Landforms: The Journal of the British Geomorphological Research Group, 34, 1726–1742, 2009.

Portenga, E. W. and Bierman, P. R.: Understanding Earth's eroding surface with 10Be, GSA Today, 21, 4–10, https://doi.org/10.1130/g111a.1, 2011.

Portenga, E. W., Bierman, P., Duncan, C., Corbett, L. B., Kehrwald, N. M., and Rood, D. H.: Erosion rates of the Bhutanese Himalaya determined using in situ-produced 10Be, Geomorphology, 233, 112–126, https://doi.org/10.1016/j.geomorph.2014.09.027, 2015.

https://doi.org/10.5194/gchron-2024-22
Preprint. Discussion started: 28 August 2024

Repasch, M., Wittmann, H., Scheingross, J. S., Sachse, D., Szupiany, R., Orfeo, O., Fuchs, M., and Hovius, N.: Sediment Transit Time and Floodplain Storage Dynamics in Alluvial Rivers Revealed by Meteoric 10Be, Journal of Geophysical Research: Earth Surface, 125, e2019JF005419, https://doi.org/10.1029/2019JF005419, 2020.

Reusser, L., Bierman, P., and Rood, D.: Quantifying human impacts on rates of erosion and sediment transport at a landscape scale, Geology, 43, 171–174, 2015.

Reusser, L. J., Bierman, P. R., Rizzo, D. M., Portenga, E. W., and Rood, D. H.: Characterizing landscape-scale erosion using 10Be in detrital fluvial sediment: Slope-based sampling strategy detects the effect of widespread dams, Water Resources Research, 53, 4476–4486, https://doi.org/10.1002/2016WR019774, 2017.

Romans, B. W., Castelltort, S., Covault, J. A., Fildani, A., and Walsh, J.: Environmental signal propagation in sedimentary systems across timescales, Earth-Science Reviews, 153, 7–29, 2016.

Schaefer, J. M., Codilean, A. T., Willenbring, J. K., Lu, Z.-T., Keisling, B., Fülöp, R.-H., and Val, P.: Cosmogenic nuclide techniques, Nature Reviews Methods Primers, 2, 18, https://doi.org/10.1038/s43586-022-00096-9, 2022.

Schumm, S.: The Fluvial System, John Wiley & Sons, New York, 338 pp., 1977.

Struck, M., Jansen, J. D., Fujioka, T., Codilean, A. T., Fink, D., Egholm, D. L., Fülöp, R.-H., Wilcken, K. M., and Kotevski, S.: Soil production and transport on postorogenic desert hillslopes quantified with 10Be and 26Al, GSA Bulletin, 130, 1017–1040, 2018.

Tofelde, S., Bernhardt, A., Guerit, L., and Romans, B. W.: Times Associated With Source-to-Sink Propagation of Environmental Signals During Landscape Transience, Front. Earth Sci., 9, https://doi.org/10.3389/feart.2021.628315, 2021.

Vermeesch, P., Fenton, C., Kober, F., Wiggs, G., Bristow, C. S., and Xu, S.: Sand residence times of one million years in the Namib Sand Sea from cosmogenic nuclides, Nature Geoscience, 3, 862–865, 2010.

Willenbring, J. K., Codilean, A. T., and McElroy, B.: Earth is (mostly) flat: Apportionment of the flux of continental sediment over millennial time scales, Geology, 41, 343–346, https://doi.org/10.1130/g33918.1, 2013.

Wittmann, H. and von Blanckenburg, F.: Cosmogenic nuclide budgeting of floodplain sediment transfer, Geomorphology, 109, 246–256, 2009.

Wittmann, H. and von Blanckenburg, F.: The geological significance of cosmogenic nuclides in large lowland river basins, Earth-Science Reviews, 159, 118–141, 2016.

Wittmann, H., von Blanckenburg, F., Maurice, L., Guyot, J. L., and Kubik, P. W.: Recycling of Amazon floodplain sediment quantified by cosmogenic 26Al and 10Be, Geology, 39, 467–470, https://doi.org/10.1130/g31829.1, 2011.

Wittmann, H., Malusà, M. G., Resentini, A., Garzanti, E., and Niedermann, S.: The cosmogenic record of mountain erosion transmitted across a foreland basin: Source-to-sink analysis of in situ 10Be, 26Al and 21Ne in sediment of the Po river catchment, Earth and Planetary Science Letters, 452, 258–271, 2016.

Wittmann, H., Oelze, M., Gaillardet, J., Garzanti, E., and von Blanckenburg, F.: A global rate of denudation from cosmogenic nuclides in the Earth's largest rivers, Earth-Science Reviews, 204, 103147, 2020a.

Wittmann, H., Oelze, M., Gaillardet, J., Garzanti, E., and von Blanckenburg, F.: A global rate of denudation from cosmogenic nuclides in the Earth's largest rivers, Earth-Science Reviews, 204, 103147, https://doi.org/10.1016/j.earscirev.2020.103147, 2020b.